

PROJECTION-BASED REGISTRATION OF RADIOLOGICAL IMAGES¹

Çiğdem Eroğlu and A. Enis Çetin

Dept. of Electrical and Electronics Engineering,
Bilkent University, Bilkent, Ankara TR-06533, TURKEY.

Tel: (90) 312-2664307; Fax: (90) 312-2664126

e-mail: eroglu@ee.bilkent.edu.tr

ABSTRACT

This paper introduces a projection-based method for registration of radiological images. The proposed method estimates the scale, translation and rotation parameters which define the global affine motion of an image with respect to a reference image. Using these estimated parameters, radiological images can be properly re-aligned to help diagnosis. The proposed method tries to match the horizontal and vertical projections of the image to be registered with the corresponding projections of the reference image in a hierarchical manner. After coarse estimates of the parameters are obtained using low resolution images, higher resolution images are utilized for the refinement of the parameter estimates. The experiments carried out on Computed Tomography (CT) and Magnetic Resonance (MR) images show that the performance of the algorithm in estimating the affine motion parameters is encouraging.

1 INTRODUCTION

Image registration is the procedure of aligning two or more images to match the coordinates of their corresponding points [1]. In radiology, registration of volume images (CT, MRI) is often valuable for diagnosis. For example, registering CT and mammogram images taken at different times may simplify the comparison of the images for monitoring changes. Furthermore, registration is an important pre-processing step for Computer Aided Diagnosis (CAD) applications involving two or more images.

A recent paper [2] uses integral projections to reduce the computational cost of block motion estimation. In this paper, we propose an algorithm which uses 1-D projections of the images in a hierarchical way to estimate the global translation, scaling and rotation parameters between the images. In Section 2, we describe how our method estimates the scale and translation parameters of the affine transformation. In Section 3, we present our multiresolution rotation angle estimation approach and in Section 4, we present simulation examples.

¹This work was supported by the Technology Development Foundation of Turkey under TTGV-199.

2 ESTIMATION OF SCALE AND TRANSLATION PARAMETERS USING 1-D PROJECTIONS

Let $I_1(x, y)$ be our reference frame with respect to which the transformed image $I_2(x, y)$ is to be registered. The projections of $I_1(x, y)$ and $I_2(x, y)$ onto the x-axis are defined as [3, 7],

$$P_1^x(u) = \frac{1}{N_2} \sum_{y \in [1, N_2]} I_1(u, y), \quad (1)$$

$$P_2^x(u) = \frac{1}{N_2} \sum_{y \in [1, N_2]} I_2(u, y) \quad (2)$$

where N_2 denotes the y-dimension of the $N_1 \times N_2$ images. Similar expressions are also defined for the projections onto the y-axis, namely $P_1^y(u)$ and $P_2^y(u)$. Let (u_1^l, u_1^u) and (u_2^l, u_2^u) be the coordinates of the lower and upper boundaries of the one dimensional functions $P_1^x(u)$ and $P_2^x(u)$, respectively. The points u_1^l and u_1^u can be matched to the points u_2^l and u_2^u respectively using an affine transformation:

$$u_2 = S_x u_1 + T_x, \quad (3)$$

where

$$S_x = \frac{u_2^l - u_2^u}{u_1^l - u_1^u}, \quad T_x = u_2^l - \frac{u_2^l - u_2^u}{u_1^l - u_1^u} u_1^l. \quad (4)$$

The transformation (3) gives us the scale (S_x) and translation (T_x) parameters in the x-direction. Similar steps can be followed to find the scale (S_y) and translation (T_y) parameters in the y-direction.

In order to robustify the estimation procedure, one can also use other projections, including projections onto oblique lines such as,

$$P^\theta(u) = \sum_{m, n} w_\theta(m, n) I(m, n), \quad (5)$$

where $m = \lfloor u \cos \theta - y \sin \theta \rfloor$, $n = \lfloor u \sin \theta + y \cos \theta \rfloor$, θ is the angle of the line from the x-axis in the counter clockwise direction and $w_\theta(m, n)$ is the weight factor due to the line integral.

3 HIERARCHICAL PROJECTION MATCHING

We used a multiresolution technique to estimate the rotation angle around the center of the images. We first obtain the subband decomposition of the original images in both x and y directions as shown in Figure 1. The size of the resulting low resolution image $i(x, y)$ is $\frac{1}{16}$ th of the original image.

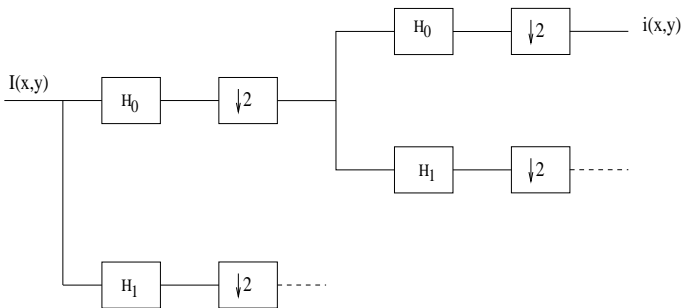


Figure 1: *Two-level subband decomposition structure.* H_0 and H_1 are low-pass and high-pass filters respectively. $I(x, y)$ is an $N_1 \times N_2$ image and $i(x, y)$ is an $\frac{N_1}{4} \times \frac{N_2}{4}$ image.

As the low-pass filter H_0 , we used a maximally-flat Lagrange filter of order seven in both dimensions [4]. The coefficients of this filter are

$$h[n] = \left[-\frac{1}{32} \quad 0 \quad \frac{9}{32} \quad \frac{1}{2} \quad \frac{9}{32} \quad 0 \quad -\frac{1}{32} \right]. \quad (6)$$

This procedure is repeated for both the reference image $I_1(x, y)$ and the transformed image $I_2(x, y)$. Using the low resolution images $i_1(x, y)$ and $i_2(x, y)$ we first search for the best candidate of the rotation angle logarithmically [5] to obtain a coarse estimate. Then we move to the next higher resolution to make the estimates of the parameters finer.

The steps of the overall algorithm are as follows:

1. Rotate the low-resolution image $i_2(x, y)$ by the angle to be tested,
2. Find the projections of $i_1(x, y)$ and $i_2(x, y)$ both in x and y directions, namely find $p_1^x(u), p_1^y(u), p_2^x(u)$, and $p_2^y(u)$),
3. Match the end points of the projections $(p_1^x(u), p_2^x(u))$ and $((p_1^y(u), p_2^y(u))$ using equations (3) and (4), to find the parameters S_x, T_x, S_y , and T_y .
4. Calculate the sums of squared error between the projections:

$$E^x |_{\theta=0} = \sum_u |p_1^x(u) - p_2^x(u)|^2, \quad (7)$$

$$E^y |_{\theta=\frac{\pi}{2}} = \sum_u |p_1^y(u) - p_2^y(u)|^2, \quad (8)$$

If the same θ does not minimize both E^x and E^y , select the θ value that minimizes the MSE between the original low resolution images $i_1(x, y)$ and $i_2(x, y)$, after $i_2(x, y)$ have been corrected by the candidate rotation angle.

5. Repeat steps (1)-(4) until the desired accuracy in the logarithmic search is achieved and select the angle θ that satisfies the conditions listed in item 4 as the estimate of the rotation angle between the images at the current resolution.
6. To obtain a finer estimate of θ , the procedure is repeated in the next higher resolution image using the present estimate of θ as our starting point. As a last step, the original images $I_1(x, y)$ and $I_2(x, y)$ are used to determine the translation, scaling and rotation parameters more accurately.

The algorithm can be improved by partially correcting the misregistered image using the rotation and scale parameters which are estimated using the lowest resolution resolution images. Then the translation parameters estimated in higher resolutions using this partly corrected misregistered image become more accurate.

Another improvement to the algorithm is to increment the accuracy of the logarithmic search by one as we step up to a higher resolution. For example, if we use 2-step logarithmic search in the lowest resolution, which provides us an accuracy of $\frac{1}{4}$ th of the current angle range, we may use 3-step logarithmic search in the next higher resolution that gives us an accuracy of $\frac{1}{8}$ th of the new angle range, which is half of the previous range. Although the computation time increases slightly, accuracy in estimation of the parameters are preferred in medical imaging.

One assumption that we made in implementing the algorithm is that the background of the images are black, which is the case for most medical images.

4 EXPERIMENTAL RESULTS

We first tested our algorithm with synthetically transformed CT images. We used the original CT image shown in Figure 2 and introduced it different affine transformations to obtain the misregistered images.

In the first example, the original image is rotated around its center by 10 degrees in the counter-clockwise direction to obtain the transformed (misregistered) image shown in Figure 2(b).

In the second example, after a rotation of 10 degrees, the image is also scaled by a factor of 0.5 in both x and y directions, which is shown in Figure 3.

In the third example, after rotation and scaling, a translation of (60,80) pixels is given to the image. This image which contains all the three possible transformations is given in Figure 4.

The steps (1)-(6) of the proposed algorithm are carried out with 2, 3, and 4-step logarithmic search in

the third, second and original resolution images, respectively. The allowable range of rotation angle is taken as $(-15, 15)$. The accuracy of the logarithmic search algorithm can be increased by increasing the number of steps in the search process or reducing the allowable range for the search.

The results using the produced CT images are given in Table 1. The estimated parameters are quite close to their actual values. The algorithm is successful even for large scale and translation transformations that we used in our experiments. Other algorithms may not be able to handle such large scale differences such as the method proposed in [6]. In order to compare our projection-based algorithm with the algorithm based on matching three different corresponding blocks of the images[6], we used the transformation parameters given in Table 2, so that the transformed image is not too much deformed and the algorithm in [6] can handle the problem. Although the block-matching-based algorithm estimated the rotation angle better than the projection-based algorithm, the translation parameters are closer to their actual values in the projection-based method. As the scale and rotation parameters become smaller, translation parameters are estimated with subpixel accuracy in the block-matching-based method.

The algorithm is also tested using two real MR images shown in Figure 5(a) and Figure 5(b). The difference of the two images before and after registration are given in Figure 5(c) and Figure 5(d), respectively. Since there is some illumination difference between the original images, the difference image after registration contains some bright areas. These real MR images are not restricted to be misregistered by an affine transformation only. Some local distortions may also exist. Since our algorithm looks for a global affine motion, these local transformations are not corrected. This is in fact a desirable property in medical image processing because we do not want to eliminate the differences resulting from anatomical changes.

5 CONCLUSION

This paper introduces a hierarchical projection-based algorithm for registration of radiological images. The algorithm is tested using both synthetically generated and real medical images. The proposed algorithm can successfully estimate the global affine motion parameters that cause the misregistration of the images even in large deformation cases.

6 ACKNOWLEDGMENT

We would like to thank A. Goshtasby of Wright State University for his permission to use the magnetic resonance images.

References

- [1] L. G. Brown, "A survey of image registration techniques", *ACM Computing Surveys*, Vol.24, pp.325-376, 1992.
- [2] K. Sauer and B. Schwartz, "Efficient Block Motion Estimation Using Integral Projections", *IEEE Transactions on Circuits and Systems for Video Technology*, Vol.6, No.5, October 1996.
- [3] **Multidimensional Digital Signal Processing**, D. Dudgeon and R. Mersereau, Prentice-Hall, New Jersey, 1984.
- [4] S. Phoong, C. W. Kim, P. P. Vaidyanathan and R. Ansari, "A new Class of Two-Channel Biorthogonal Filter Banks and Wavelet Bases", *IEEE Trans. On Signal Processing*, Vol.43, No.3, pp.649-665, 1995.
- [5] **Digital Video Processing**, M. Tekalp, Prentice-Hall, New Jersey, 1995.
- [6] Ç. Eroğlu, A. T. Erdem, "A Fast Algorithm for Subpixel Accuracy Image Stabilization for Digital Film and Video", *SPIE-Visual Communications and Image Processing'98*, Vol.3309, pp.786-797, 1998.
- [7] **Basic Methods of Tomography and Inverse Problems**, G. Herman, H. K. Tuy, K. J. Langenberg and P. C. Sabatier, IOP Publishing Limited, 1987.

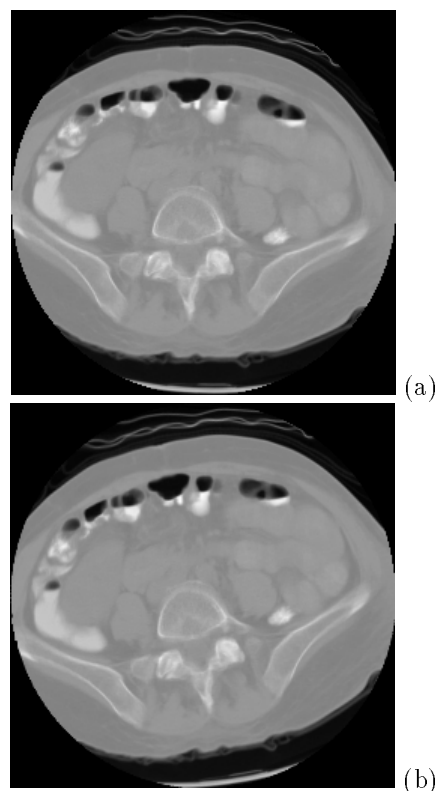


Figure 2: (a) The reference CT image. (b) The 10 degree rotated CT image.

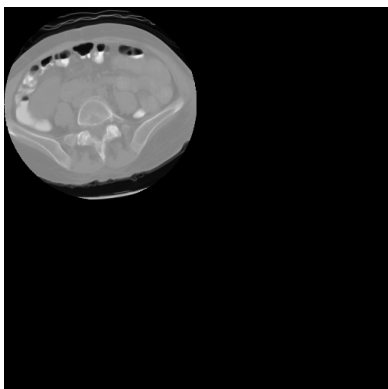


Figure 3: The image rotated by 10 degrees in the counter-clockwise direction and then scaled by 0.5 in both x and y dimensions.

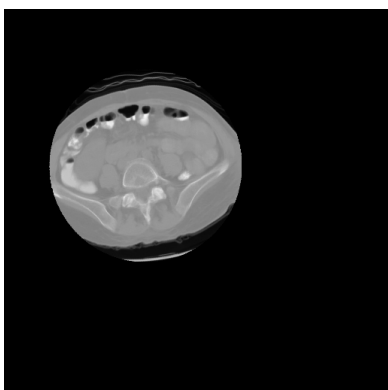


Figure 4: The image rotated by 10 degrees in the counter clockwise direction, scaled by 0.5 in both x and y dimensions, and then translated by $(60, 80)$ pixels.

Actual transformation parameters					
	θ	S_x	S_y	T_x	T_y
R	10	1	1	0	0
R,S	10	0.5	0.5	0	0
R,S,T	10	0.5	0.5	60	80
Estimated parameters					
	$\hat{\theta}$	\hat{S}_x	\hat{S}_y	\hat{T}_x	\hat{T}_y
R	10.0781	1	1	0	0
R,S	9.4922	0.4894	0.5056	2	-1
R,S,T	10.0781	0.5056	0.5036	59	79

Table 1: The simulation results using the CT image. R , S and T denote the existence of rotation, scale and translation. The hats on the parameters denote the estimated values.

Actual transformation parameters					
	θ	S_x	S_y	T_x	T_y
R	10	1	1	0	0
R,S,T	10	0.9	0.9	5	10
R,S,T	5	0.95	0.95	5	10
Estimated parameters, Projection-based method					
	$\hat{\theta}$	\hat{S}_x	\hat{S}_y	\hat{T}_x	\hat{T}_y
R	10.0781	1	1	0	0
R,S,T	9.84375	0.9069	0.9017	4	11
R,S,T	5	0.9575	0.9515	3	11
Estimated parameters, Block-matching-based method					
	$\hat{\theta}$	\hat{S}_x	\hat{S}_y	\hat{T}_x	\hat{T}_y
R	10.0124	1	1	0.0250	-0.681
R,S,T	10.0124	0.9002	0.8994	6.39	8.86
R,S,T	4.9926	0.9500	0.9499	5.51123	9.7441

Table 2: The simulation results using the CT image. R denotes rotation, S denotes scale and T denotes translation. The hats on the parameters denote the estimated values.

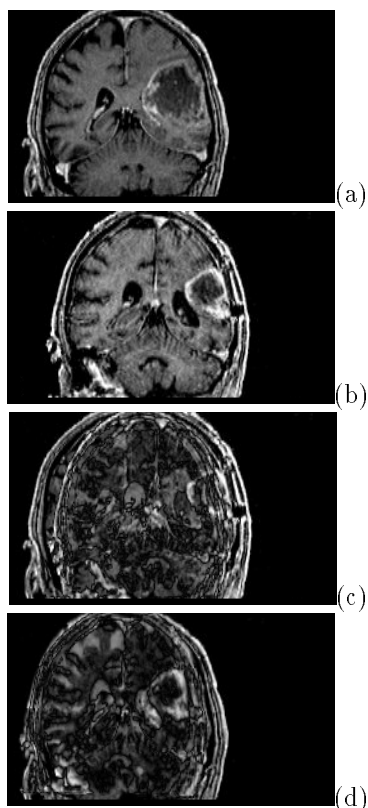


Figure 5: (a),(b) Serial MR images of a brain with a tumor. (c) Difference image before registration. (d) Difference image after registration.